Fasting exacerbates hepatic growth differentiation factor 15 to promote fatty acid β-oxidation and ketogenesis via activating XBP1 signaling in liver

Meiyuan Zhang, Weilan Sun, Jin Qian, Yan Tang*

Emergency Intensive Care Unit, Qingpu Branch of Zhongshan Hospital, Fudan University, Shanghai 201700, China

ARTICLE INFO

ABSTRACT

Liver coordinates a series of metabolic adaptations to maintain systemic energy balance and provide adequate nutrients for critical organs, tissues and cells during starvation. However, the mediator(s) implicated in orchestrating these fasting-induced adaptive responses and the underlying molecular mechanisms are still obscure. Here we show that hepatic growth differentiation factor 15 (GDF15) is regulated by IRE1α-XBP1s branch and promotes hepatic fatty acids β-oxidation and ketogenesis upon fasting. GDF15 expression was exacerbated in liver of mice subjected to long-term fasted or ketogenic diet feeding. Abrogation of hepatic *Gdf15* dramatically attenuated hepatic β-oxidation and ketogenesis in fasted mice or mice with STZ-initiated type I diabetes. Further study revealed that XBP1s activated *Gdf15* transcription via binding to its promoter. Elevated GDF15 in liver reduced lipid accumulation and impaired NALFD development in obese mice through enhancing fatty acids oxidation in liver. Therefore, our results demonstrate a novel and critical role of hepatic GDF15 activated by IRE1α-XBP1s branch in regulating adaptive responses of liver upon starvation stress.

1. Introduction

During starvation, liver coordinates a series of metabolic adaptations to maintain systemic energy balance and provide adequate nutrients for critical organs, tissues and cells [1]. These adaptive responses in liver are well orchestrated including supplying glucose to the circulation initially from hepatic glycogen followed by gluconeogenesis produced by other noncarbohydrate materials. In sustained fasting state, ketones are synthesized by liver and provide an alternative energy source instead of glucose for highly oxidative tissues [2]. Hepatic fatty acid β-oxidation is considered to be critical for these processes for providing ATP and NADP to facilitate gluconeogenesis and acetyle-CoA for ketogenesis [3]. Accumulative studies reveal plenty of molecular taking part in regulating hepatic β-oxidation during fasting or other physiological states, including peroxisome proliferator-activated receptor alpha (*Ppara*) [4], fibroblast growth factor 21 (*Fgf21*) [5]. It is still valuable to discover novel mediator(s) to further understand the regulation of hepatic fatty acid β-oxidation and ketogenesis.

Growth differentiation factor 15 (GDF15), also known as MIC-1, is a member of the transforming growth factor-β (TGF-β)/bone morphogenetic protein (BMP) super family and a secreted protein circulating in plasma as a 25-kDa homodimer [6,7]. GDF15 is found to be highly expressed in the placenta and prostate and also in heart, pancreas, liver, kidney and colon [8–10]. Notably, Circulating GDF15 are increased in obese and type 2 diabetic patients and display high correlation with body mass index (BMI), body fat, glucose, and C-reactive proteins, indicating its crucial functions in the pathogenesis of metabolic diseases [11]. GDF15 is wildly accepted as a biomarker and higher levels are closely associated with increased risk of cardiovascular disease [12,13]. GDF15 is implicated in governing systemic energy balance and protecting against obesity through enhancing thermogenesis and oxidative metabolism [14,15]. However, physiological roles of GDF15 in hepatic lipid homeostasis and underlying molecular mechanism(s) are still obscure.

Accumulation of unfolded or misfolded proteins in lumen of endoplasmic reticulum causes ER stress and subsequently activates the cellular unfolded protein response (UPR) [16,17]. Mammalian UPR pathways are composed of three branches which are initiated by ER membrane-located proteins, including activating transcription factor 6 (ATF6), inositol requiring enzyme 1 (IRE1), and double-stranded RNA-activated protein kinase-like ER kinase (PERK). Among the UPR pathways, IRE1α-XBP1 branch is the most conserved one, indicating its

essential role in cells [16–18]. Upon activation, IRE1α catalyzes the non-conventional splicing of the mRNA encoding X-box-binding protein 1 (XBP1) by removing 26nt intron, and thereby products an active spliced form (XBP1s) to initiated a key UPR program [19]. Growing studies in animal models have revealed the crucial role of IRE1α or XBP1s in both glucose and lipid metabolism [20–26]. Although several studies implicate IRE1a-XBP1s in lipid homeostasis of liver in fasted mice [20,21], it still remains largely elusive how IRE1α-XBP1s branch acts in regulating hepatic lipid metabolism under physiological conditions. Here we present that hepatic GDF15 which is controlled by IRE1α-XBP1s branch could be upregulated and promote fatty acids β-oxidation and ketogenesis of liver during fasting.

2. Materials and methods

2.1. Animals

C57BL/6 J wild type mice were obtained from Shanghai Laboratory Animal Co. Ltd. (SILAC) and housed in laboratory cages at a temperature of $23 \pm 3\,°C$ with a humidity of $35 \pm 5\%$ under 12-h dark/light cycle (lights on at 7:00 a.m.).

For fed and fasting experiments, fasted mice were kept from food (regular chow diet) for 24 h and sacrificed within 2 h after lights on; mice fed *al libitum* were free to access to food and sacrificed at the same time of the day as fasted mice. For diet-induced ketogenesis studies, mice were fed with a ketogenic diet (containing 17.6% protein, 0.2% carbohydrate and 57.2% fat, w/w, Research Diets Inc., #D12369B) for 3 days and sacrificed within 2 h after lights on.

For diabetic ketoacidosis, mice were firstly administered with adenovirus of ad-NC and ad-siGfp15 as indicated, respectively. Two weeks later, these mice were injected intraperitoneally (i.p.) with streptozotocin (STZ, Sigma-Aldrich, #S0130) at a dose of 250 mg per Kg body weight as previously described [21] and sacrificed within 2 h after lights on. All experiments in this study were performed in accordance with protocols approved by the Institutional Animal Care and Use Committee of Fudan University.

2.2. Serum and liver measurements

Hepatic levels of TGs, Cholesterol and FFAs were respectively determined using the triglyceride determination kit (Sigma, triglyceride reagent #T2449 and free glycerol reagent #F6428), Cholesterol assay kit (Sigma, Cholesterol Quantitation KitMAK043-1KT), FFA assay kit (Cayman Chemical, #700310), all according to manufacturers' instructions. Serum and hepatic GFD15 was determined using ELISA kit (R&D System, #MGD150).

For measurement of hepatic TG, FFA and Cholesterol, $\sim 30\,mg$ of liver tissue was homogenized in 0.5 ml PBS. After sufficient mixing of 0.4-ml homogenates with 1.6 ml of CHCl3-CH3OH (2:1, v/v), the suspension was centrifuged at 3,000 rpm for 10 min at room temperature and then the lower organic phase was transferred for air-dried overnight in a chemical hood. The residual liquid was re-suspended in 400 µl of ethanol with 1% Triton X-100. TG contents were determined using the triglyceride determination kit (Sigma, triglyceride reagent #T2449 and free glycerol reagent #F6428). Cholesterol contents were determined using the Cholesterol Assay Kit (Sigma, Cholesterol Quantitation Kit #MAK043-1KT). For determining hepatic levels of GDF15, liver tissues were firstly homogenized in the homogenization buffer (0.01 N HCl, 1 mM EDTA, 4 mM $Na_2S_2O_5$), and then centrifuged at 13,000 rpm for 15 min at 4 °C to remove the cellular debris. The homogenates were collected and stored at $-80\,°C$ prior to measurement by ELISA. For determining secreted GDF15, cell culture medium (3 ml) was collected as indication. Then the supernatant was concentrated to 200 µl by the using of an Amicon Ultra-4 centrifugal filter unit (Millipore). GDF15 was measured using the ELISA kit (R&D System, #MGD150) according to the manufacturer's instructions.

2.3. Isolation of primary hepatocytes of mice

Primary hepatocytes were isolated from male mice at 8–12 weeks of age as previously described [21]. Briefly, collagenase perfusion was performed with 50 ml of perfusion buffer through the portal vein of mice after anesthetizing. Livers were aseptically removed and minced in a sterile 10-cm cell culture dish with ice-cold perfusion buffer without collagenase. Then, hepatocytes were filtrated through a 70 µm cell strainer (BD Falcon) into a new tube followed with centrifugation at 50 g for 2 min at 4 °C. Cells were then washed with cold hepatocyte wash medium (Invitrogen) three times and re-suspended in 15 ml of cold HepatoZYME-SFM medium (Invitrogen) supplemented with 2 mM L-glutamine, 20 units/ml penicillin, and 20 µg/ml streptomycin. After trypan blue staining for determination of viability, cells were plated at 6×10^5 cells/well in 6-well culture dishes or at 3×10^5 cells/well in 12-well dishes pre-coated with collagen. Cells were cultured for at least 8 h before further use. Cells were subsequently treated with the desired reagents prior to further analysis.

2.4. Quantitative real-time RT-PCR analysis

Total RNAs were isolated from cells or liver tissues by TRIzol reagent (Invitrogen), and cDNA was generated by M-MLV reverse transcriptase with random hexamer primers (Invitrogen). Quantitative Real-time PCR (qRT-PCR) was performed with an ABI Prism 7500 sequence detection system, using the SYBR Green PCR Master Mix (Applied Biosystems). Ct values were normalized to mouse *Rps18* levels using the ΔΔ-Ct method. The sequences of primers mainly used in this study showed as following.

Rpl18: sense 5′-ATGATGTGCGGATTCTGGAAG-3′, antisense5′- CCT GGGGGCCTTGCCAAAAT-3′;

Gdf15: sense 5′- CTGGCAATGCCTGAACAACG-3′, antisense 5′- GGTCGGGACTTGGTTCTGAG-3′;

Ppara: sense 5′-AGAGCCCCATCTGTCCTCTC-3′, antisense 5′-ACTG GTAGTCTGCAAAACCAAA-3′;

Fgf21: sense 5′-CTGCTGGGGGTCTACCAAG-3′, antisense 5′- CTGC GCCTACCACTGTTCC-3′;

Acadl: sense 5′-TCTTTTCCTCGGAGCATGACA-3′, antisense 5′- GAC CTCTCTACTCACTTCTCCAG-3′;

Acox1: sense 5′-TAACTTCCTCACTCGAAGCCA-3′, antisense 5′-AGTTCCATGACCCATCTCTGTC-3′;

Cpt1a: sense 5′-CTCCGCCTGAGCCATGAAG-3′, antisense 5′- CACC AGTGATGATGCCATTCT-3′;

Hmgcs2: sense 5′-CTCCGCCTGAGCCATGAAG-3′, antisense 5′- CAC CAGTGATGATGCCATTCT-3′;

Pparg: sense 5′-TCGCTGATGCACTGCCTATG-3′, antisense 5′- GAG AGGTCCACAGAGCTGATT-3′;

Hsl: sense 5′-GATTTACGCACGATGACACAGT-3′, antisense 5′- ACC TGCAAAGACATTAGACAGC-3′;

Atgl: sense 5′-CTGAGAATCACCATTCCCACATC-3′, antisense 5′-CACAGCATGTAAGGGGGAGA-3′;

Xbp1s: sense 5′-CTGAGTCCGAATCAGGTGCAG-3′, antisense 5′-GTC CATGGGAAGATGTTCTGG-3′;

Bip: sense 5′-ACTTGGGGACCACCTATTCCT-3′, antisense 5′- ATCG CCAATCAGACGCTCC-3′;

Chop: sense 5′-CTGGAAGCCTGGTATGAGGAT-3′, antisense 5′-CAGGGTCAAGAGTAGTGAAGGT −3′;

Erdj4: sense 5′-ATAAAAGCCCTGATGCTGAAGC-3′, antisense 5′-GCCATTGGTAAAAGCACTGTGT-3′;

Fasn: sense 5′-GGCTCTATGGATTACCCAAGC-3′, antisense 5′-CCAG TGTTCGTTCCTCGGA-3′;

Scd1: sense 5′-AGATCTCCAGTTCTTACACGACCAC-3′, antisense 5′-GACGGATGTCTTCTTCCAGGTG-3′;

Pgc1a: sense 5′-TATGGAGTGACATAGAGTGTGCT-3′, antisense 5′-CCACTTCAATCCACCCAGAAAG-3′;

Acc1: sense 5′-GATGAACCATCTCCGTTGGC-3′, antisense 5′-CCCA

ATTATGAATCGGGAGTGC-3′;

Cd36: sense 5′-GAACCACTGCTTTCAAAAACTGG-3′, antisense 5′-TGCTGTTCTTTGCCACGTCA-3′;

ApoB: sense 5′-GCTCAACTCAGGTTACCGTGA-3′, antisense 5′-AGAGGGCTGACACTTGTACTG-3′;

Srebp1c: sense 5′-GGAGCCATGGATTGCACATT-3′, antisense 5′-GGCCCGGGAAGTCACTGT-3′;

Pparg: sense 5′-TCGCTGATGCACTGCCTATG-3′, antisense 5′-GAGAGGTCCACAGAGCTGATT-3′;

ApocIII: sense 5′-TACAGGGCTACATGGAACAAGC-3′, antisense 5′-CAGGGATCTGAAGTGATTGTCC-3′.

2.5. Luciferase reporter assays

The luciferase (Luc) reporter plasmids for mouse GDF15 promoter spanning the region from −1998 to +3 were constructed in pGL3 (Promega) utilizing a PCR-based cloning strategy. For luciferase activity assays, HEK293T ells were co-transfected with the *Gdf15* promoter-Luc and β-galactosidase plasmids before treatment with thapsigargin (Tg, 1 μM) or tunicamycin (Tm, 5 μg/ml) for 6 h, or co-transfected with the Luc reporter plasmid, pCMV-CHOP and β-galactosidase plasmids. Luciferase activity was measured by the using of Dual-Luciferase Reporter Assay System (Promega) following the manufacturer's instructions, and β-galactosidase activity was used for normalization.

2.6. Chromatin immunoprecipitation (ChIP)

ChIP assays were performed with the Agarose ChIP Kit (Pierce, Thermo Fisher) according to the manufacturer's instructions. In brief, cells or liver tissues were subjected to cross-linking with 1% formaldehyde before the preparation of nuclear extracts. Chromatin-CHOP complexes were immunoprecipitated with normal rabbit IgG or anti-CHOP antibodies (Cell Signaling Technology) by incubation at 4 °C overnight on a rocking platform, and then incubated with the beads from the ChIP kit at 4 °C for 2 h with gentle rocking. After washing sufficiently with the washing buffer, the complexes were eluted with the elution buffer from the beads and were subjected to further PCR analysis.

2.7. Histology analysis

Liver were harvested from indicated mice after perfusion (4% paraformaldehyde) and fixed in 4% paraformaldehyde for at least 72 h and then embedded in paraffin before cut into 5 μm sections for being stained with hematoxylin and eosin (H&E).

For Oil-Red O staining, frozen liver sections (10 μm) were rinsed with 60% isopropanol and then applied to stain with freshly prepared Oil-red O solution (Sigma) for 10 min. The sections were then rinsed again with 60% isopropanol, and nuclei were stained with alum hematoxylin before analysis by microscopy.

For Masson's trichrome staining, formalin-fixed, paraffin-embedded sections of livers were applied to use the Trichrome Stain Kit (Abcam, #ab150686), according to manufacturers' instructions.

2.8. Immunoblotting analysis

Immunoblotting was performed as previous described [21]. Briefly, frozen liver tissues were homogenized for dissecting in RIPA lysis buffer added with protease inhibitors (Sigma). After centrifuging, the supernatant was collected and incubated in 100 °C with the addition of loading buffer for 10 min. When firstly separated by SDS-PAGE, proteins in the gel were transferred to polyvinylidene difluoride (PVDF) membrane. Subsequently, the membranes were incubated in 10% fat-free milk for 1 h. For primary antibodies incubation, membranes were respectively subjected to an overnight incubation with the antibodies against p-IRE1α (1:500, Novus Biologicals), IRE1α (1:2000, Cell

Signaling Technology), p-eIF2α (1:1000, Cell Signaling Technology), eIF2α (1:2000, Cell Signaling Technology), p-ATK (1:1000, Cell Signaling Technology), AKT (1:2000, Cell Signaling Technology) or GAPDH (1:5000, Abcam) at 4 °C, following with incubation in horseradish peroxidase-conjugated secondary antibodies. Proteins were detected by enhanced chemiluminescence assay (Thermo Fisher Scientific).

2.9. Statistical analysis

All data are presented as the mean ± standard errors of the mean (s.e.m.). Statistical analysis was conducted using unpaired two-tailed student's *t*-test, one-way or two-way analysis of variance (ANOVA), followed by Bonferroni's posttest with GraphPad Prism 5.0. *P* values < 0.05 were considered to be statistically significant.

3. Results

3.1. GDF15 expression is augmented in liver of mice upon fasting and ketogenic diet feeding

To explore if hepatic GDF15 playing a role in adaptive response of liver upon fasting, we firstly examined the expression levels of *Gdf15* in the livers of mice that were subjected to 24-h fasting. Impressively, relative to fed mice, livers of fasted mice exhibited about 6-fold increase of *Gdf15* mRNA abundance (Fig. 1A). Furthermore, GDF15 concentrations were elevated in both circulation (∼ 3-fold, Fig. 1B) and liver (∼ 15-fold, Fig. 1C) of mice subjected to 24-h fasting. In comparison to fed mice, *Gdf15* expression in other major tissues or organs, including gonadal adipose tissue, skeletal muscle, heart, lung, brain and kidney, didn't show any changes in fasted mice, indicating that increased circulating GDF15 of fasted mice were derived from liver (Fig. S1A).

As long term fasting initiates ketones production in liver, we next maintained mice with ketogenic diet feeding to investigate the role of hepatokine GDF15 in ketogenesis. Consistently, 3-day ketogenic diet (KD) feeding of mice induced robust exacerbation of *Gdf15* mRNA in liver (∼ 20-fold, Fig. 1D), rather than other major tissues or organs (Fig. S1B). Secreted GDF15 into circulation (∼ 5-fold) and hepatic contents of GDF15 (∼ 3-fold) were extremely increased in KD-feeding mice (Fig. 1E–F). Together, these results demonstrate that hepatic GDF15 could be induced in the livers of mice upon long term starvation and KD feeding, suggesting the importance of GDF15 in response to fasting stress.

3.2. XBP1s regulates hepatic Gdf15 expression

Previous study demonstrated that IRE1α-XBP1 branch of the UPR pathways is activated in the liver of fasted mice and drives the expression of *Ppara* to orchestrate hepatic β-oxidation and ketogenesis [21]. Consistently, we found obviously enhanced activation of IRE1α rather than eIF2α in fasted livers in comparison with fed group (Fig. S2A). What's more, significant increases of *Xbp1* mRNA splicing and its direct target gene (*Erdj4*) but not mRNA levels of *Bip* or *Chop* in the livers of our mice after fasting or ketogenic diet feeding, indicating increased activation of IRE1α-XBP1s branch of the UPR pathways (Fig. S2B–C). Therefore, we postulated that heightened XBP1s takes part in the regulation of *Gdf15* in fasted liver. Impressively, mRNA levels of *Gdf15* were robustly exaggerated in mouse primary hepatocytes infected with adenovirus (ad-XBP1s) to enforce XBP1s levels (Fig. 2A). To investigate if XBP1s could increase *Gdf15* expression in vivo, we enforced XBP1s expression in livers of mice via injection of ad-XBP1s. With increased XBP1s, ad-XBP1s-administered mice displayed markedly higher levels of hepatic *Gdf15* mRNA (Fig. 2B) and proteins (Fig. 2C), as well as the contents of serum GDF15 (Fig. 2D).

To explore the underlying molecular details of XBP1s regulating *Gdf15* expression, we analyzed the potential promoter sequence of
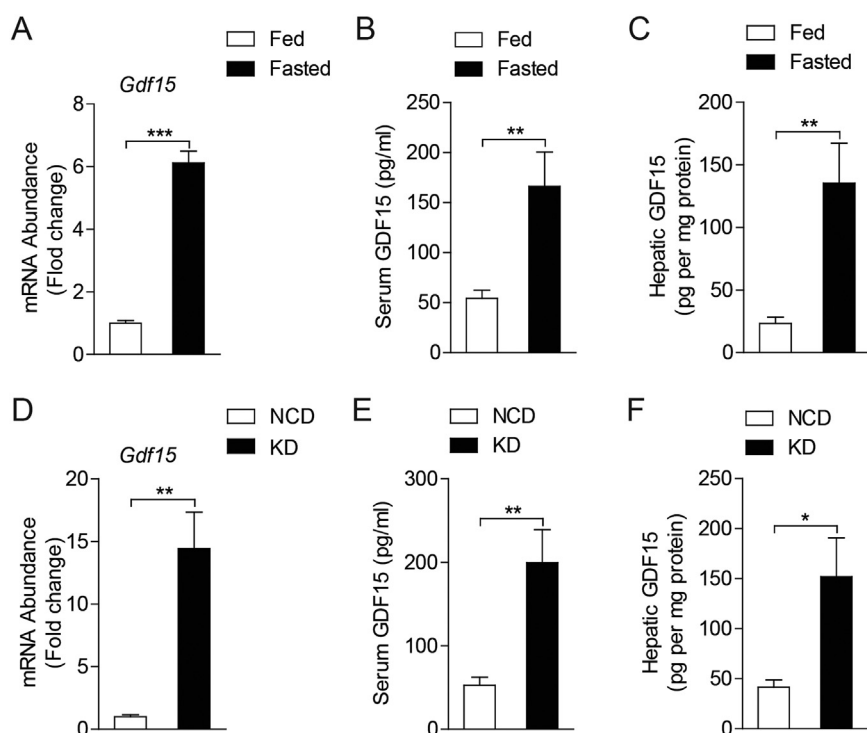
Fig. 1. Hepatic GDF15 is augmented in liver of mice upon fasting and ketogenic diet feeding. (A-C) C57BL/6 J mice were subjected to fasting for 24 h (Fasted, n = 10) or feeding freely (Fed, n = 10). A, qRT-PCR analysis of *Gdf15* mRNA levels in liver. *Rps18* was used as the internal control. B-C, ELISA assays determined the contents of serum GDF15 (B) and hepatic GDF15 (C). (D-F) C57BL/6 J mice were maintained on normal chow diet (NCD) or ketogenic diet (KD) for 3 days (n = 8 per group). (Fasted, n = 8) or feeding freely (Fed, n = 8). D, qRT-PCR analysis of *Gdf15* mRNA levels in liver. E-F, ELISA assays determined the contents of serum GDF15 (E) and hepatic GDF15 (F). For A and D, *Rpl18* was used as the internal control. All data are shown as mean ± s.e.m.. *, $p < .05$; **, $p < .01$ or ***, $p < .001$ by unpaired two-tailed Student's *t*-test.

mouse *Gdf15*. A putative ER stress-response element (ERSE) CCATT…N (n)…CCACG, was identified in the promoter sequence of mouse (Fig. 2E), which was a potential XBP1s-binding core site as previously reported [27,28]. Thus, luciferase reporter plasmids were constructed to evaluate the importance of this core site, which contain mouse *Gdf15* promoter of full length (WT) or "CCATT" deletion (ΔCCATT). In the results of luciferase assays performed in HEK293T cells, the transcriptional activities of *Gdf15* promoter were dramatically enhanced when XBP1s were overexpressed but were almost abolished when "CCATT" core sequence was deleted (Fig. 2F). Next, we conducted chromatin immunoprecitation (ChIP) assays to determine whether XBP1s could bind directly to *Gdf15* promoter. Interestingly, exogenous Flag-tagged XBP1s protein were co-immunoprecipitated with DNA of *Gdf15* promoter in primary hepatocytes (Fig. 2G). Further investigation revealed that after the deletion of "CCATT" core sequence (ΔCCATT), XBP1s proteins lost the interaction with *Gdf15* promoter as shown of the result of ChIP performed in HEK293T cells (Fig. 2H). Additionally, the efficiency of XBP1s binding to *Gdf15* promoter were significantly enhanced in liver of mice after 24-h fasting (Fig. 2I). Together, these results reveal that XBP1s could directly bind to the *Gdf15* promoter and activate its transcription in fasted liver.

3.3. Abrogation of hepatic GDF15 impairs fatty acid β-oxidation and ketogenesis in fasted mice

During extended periods of food deprivation, the liver is known to undergo metabolic reprogramming to oxidize fatty acids and produce ketones for the brain and other tissues as the primary energy source [21]. To investigate whether fasting-induced hepatic GDF15 is critical in regulating fatty acid β-oxidation and ketone production of liver, we applied adenovirus expressing siRNA specially targeted at mouse *Gdf15* mRNA (ad-siGdf15) to inhibit GDF15 expression in liver rather than other major tissues or organs (Fig. 3G, Fig. S1C), and eventually resulted in dramatic reduction of serum GDF15 contents (Fig. 3I), which further confirmed that fasting-upregulated GDF15 in circulation are mainly produced by liver. Ad-siGdf15-injected mice exhibited massive accumulation of lipids (Figs. 3A and 2B) and markedly increased hepatic triglyceride (TG) contents (Fig. 3C) in the livers of 24-h fasting.

Impressively, decreased hepatic GDF15 resulted in significant reduction of fasting-upregulated serum β-hydrobutyrate, indicating possible defects in ketogenic output of liver (Fig. 3D). Moreover, relative to mice of ad-NC, liver extracts of fasted ad-siGdf15-administered mice displayed dramatically decreased β-oxidation activity (Fig. 3E). Fasted animals administered with ad-siGdf15 also have a severe reduction in their ability to produce ketones (β-hydroxybutyrate) when treated octanoate, a ketogenic substrate with high mitochondria permeability (Fig. 3F) [29]. Further studies also demonstrate that loss of hepatic GDF15 resulted in marked decreases of mRNA levels of key genes involved in hepatic fatty acid β-oxidation and ketogenesis, including *Ppara*, *Peroxisome proliferator-activated receptor γ coactivator 1α (Pgc1a)*, *Acyl-Coenzyme A dehydrogenase (Acadl)*, *Acyl-Coenzyme A oxidase 1 (Acox1)*, *Carnitine palmitoyltransferase 1a (Cpt1a)* and *3-hydroxy-3-methylglutaryl-Coenzyme A synthase 2 (Hmgcs2)* (Fig. 3G), but showed no impacts on expression levels of other genes involved in liver metabolism, such as lipogenesis, fatty acid uptake and vLDL secretion (Fig. 3H). Interestingly, ad-siGdf15-treated mice displayed reduction of fasting-induced free fat acids (FFA) in circulation (Fig. 3J) and downregulated expression levels of lipolysis-associated genes (*Hormone sensitive lipase (Hsl)* and *Adipose triglyceride lipase (Atgl)*) in gWAT (Fig. 3K), indicating that impaired hepatic GDF15 attenuate lipolysis in white adipose tissue. These data implicate that hepatic GDF15 is of great importance in fasting-induced fatty acid β-oxidation and ketogenesis.

3.4. Abrogation of hepatic GDF15 reduces diet-induced ketogenesis and alleviates ketoacidosis of diabetic mice

To determine the role of GDF15 in ketogenesis of liver, we fed the mice with a ketogenic diet (KD) to enforce hepatic ketones production in liver. Relative to feeding a normal chow diet (NCD), KD consumption for 3 days efficiently caused excess lipid accumulation in liver (Fig. 4A-C) and extremely upregulated serum content of β-hydroxybutyrate (Fig. 4D). After ad-siGdf15-mediated ablation of hepatic GDF15 (Fig. 4E), KD-feeding mice displayed much more TGs content in the liver but dramatic reduction of serum ketones (Fig. 4A-D). Moreover, decreased hepatic GDF15 also repressed expression levels of genes involved in fatty acid β-oxidation and ketogenesis in livers, including
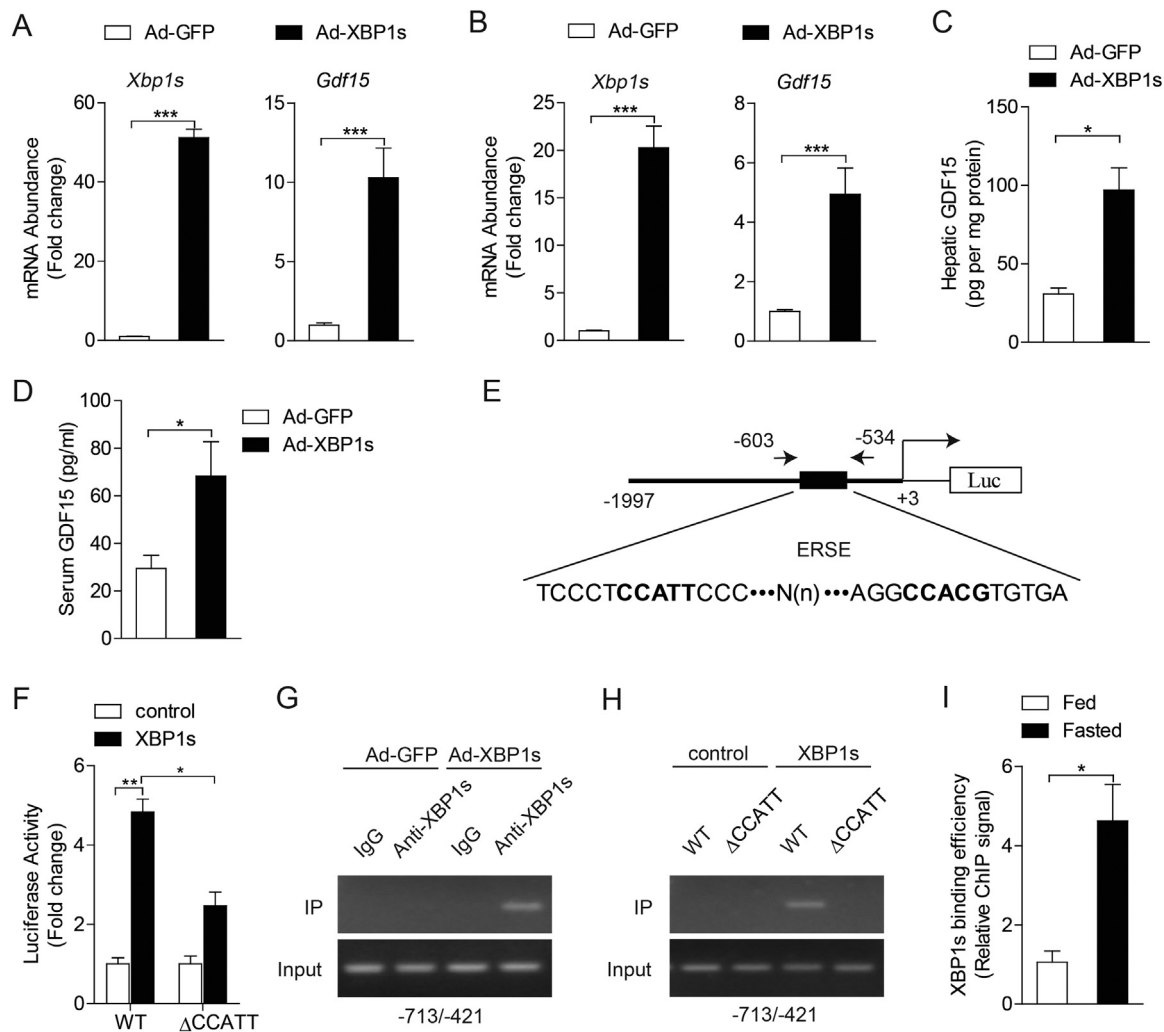
Fig. 2. XBP1s activates transcriptional activity of the *Gdf15* promoter. A Mouse primary hepatocytes were transfected with adenovirus expressing GFP (Ad-GFP) or XBP1s (Ad-XBP1s). qRT-PCR analysis of *Xbp1* splicing (*Xbp1s* normalized to total *Xbp1*) and *Gdf15* mRNA abundance. B-D, C57BL/6 J mice were administered with ad-GFP and ad-XBP1s (n = 6 per group). B, qRT-PCR analysis of *Xbp1* splicing and *Gdf15* mRNA abundance in liver. C-D, Hepatic contents (C) and Serum contents (D) of GDF15. E, Analysis of mouse *Gdf15* promoter. The region that contains the signature XBP1s-binding element (ERSE) is indicated by black boxes. F, Luciferase reporter assay. HEK293T cells were co-transfected with control vector (control) or pCDNA3.1-XBP1s plasmids (XBP1s) together with Luc constructs under the control of the mouse *Gdf15* promoter (WT) or that with the CCATT element deleted (ΔCCATT). G, Chromatin immunoprecipitation assay. Primary hepatocytes were infected with ad-GFP and ad-XBP1s and ChIP was performed 2 days later using IgG as control or XBP1s antibody (anti-XBP1s). Shown is the PCR amplification of the indicated region (from −713 to −24 upstream of the transcription start site). H, ChIP assay. Nuclear extracts were prepared from HEK293T cells co-transfected with control vector (control) or pCDNA3.1-XBP1s (XBP1s) plasmid combined with the WT or CCATT mutant reporter construct. ChIP was performed using XBP1s antibodies. Shown is the PCR amplification of the indicated region. I, ChIP assay. Nuclear extracts were prepared from liver of mice subjected to 24-h fasting or fed by the using of XBP1s antibodies (n = 5 per group). Shown is the result of qRT-PCR. All data are shown as mean ± s.e.m.. *, $p < .05$; **, $p < .01$ or ***, $p < .001$ by unpaired two-tailed Student's *t*-test or two-way ANOVA.

Ppara, Acadl, Acox1, Cpt1a and *Hmgcs2* (Fig. 4E).

Subsequently, we applied streptozotocin (STZ)-induced type 1 diabetic mice as another kind of ketotic model [30] to further investigate physiological roles of hepatic GDF15 in liver ketogenesis. First of all, at 3 days after STZ injection, mice with non-fasting blood glucose levels higher than 300 mg/dl and almost none circulating insulin were selected for further analysis (Fig. 5A and B). In consisting with previous study [21], STZ treatment dramatically enlarged *Xbp1* mRNA splicing levels in liver (Fig. 5C). Importantly, hepatic *Gdf15* mRNA abundance also showed greatly upregulated after STZ treatment and was significantly suppressed when ad-siGdf15 were injected (Fig. 5C). Indeed, levels of serum β-hydroxybutyrate were greatly elevated in STZ-treated mice but significantly repressed after the loss of hepatic GDF15, indicating impairment of ketone production in Gdf15-abrogated liver (Fig. 5D). Consistently, reduced hepatic GDF15 repressed expression levels of genes involved in fatty acid β-oxidation and ketogenesis in livers of STZ-treated mice, including *Ppara, Acadl, Acox1, Cpt1a* and

Hmgcs2 (Fig. 5E). To investigate whether insulin could correct changes of hepatic *Gdf15* expression, we treated the STZ-induced diabetic mice with insulin. Interestingly, insulin treatment efficiently repressed the upregulated *Xbp1* splicing and *Gdf15* mRNA levels in livers of STZ-treated mice (Fig. S4A-B), and then reduced the elevated β-hydoxybutyrate in blood (Fig. S4C).

3.5. Elevated hepatic GDF15 reduces hepatosteatosis and improves insulin resistance via enhancing lipid catabolism in obese mice

To explore whether GDF15 plays a role in the development of obesity-induced fatty liver, we analyzed GDF15 expression in the livers of leptin receptor-deficient mice (*db/db* mice). Interestingly, relative to control littermates (WT), *db/db* mice displayed dramatic increases of hepatic *Gdf15* mRNA abundance and protein levels in circulation and liver (Fig. S5A-C). To further explore physiological functions of GDF15 in NAFLD, *db/db* mice were injected with adenovirus expressing GFP
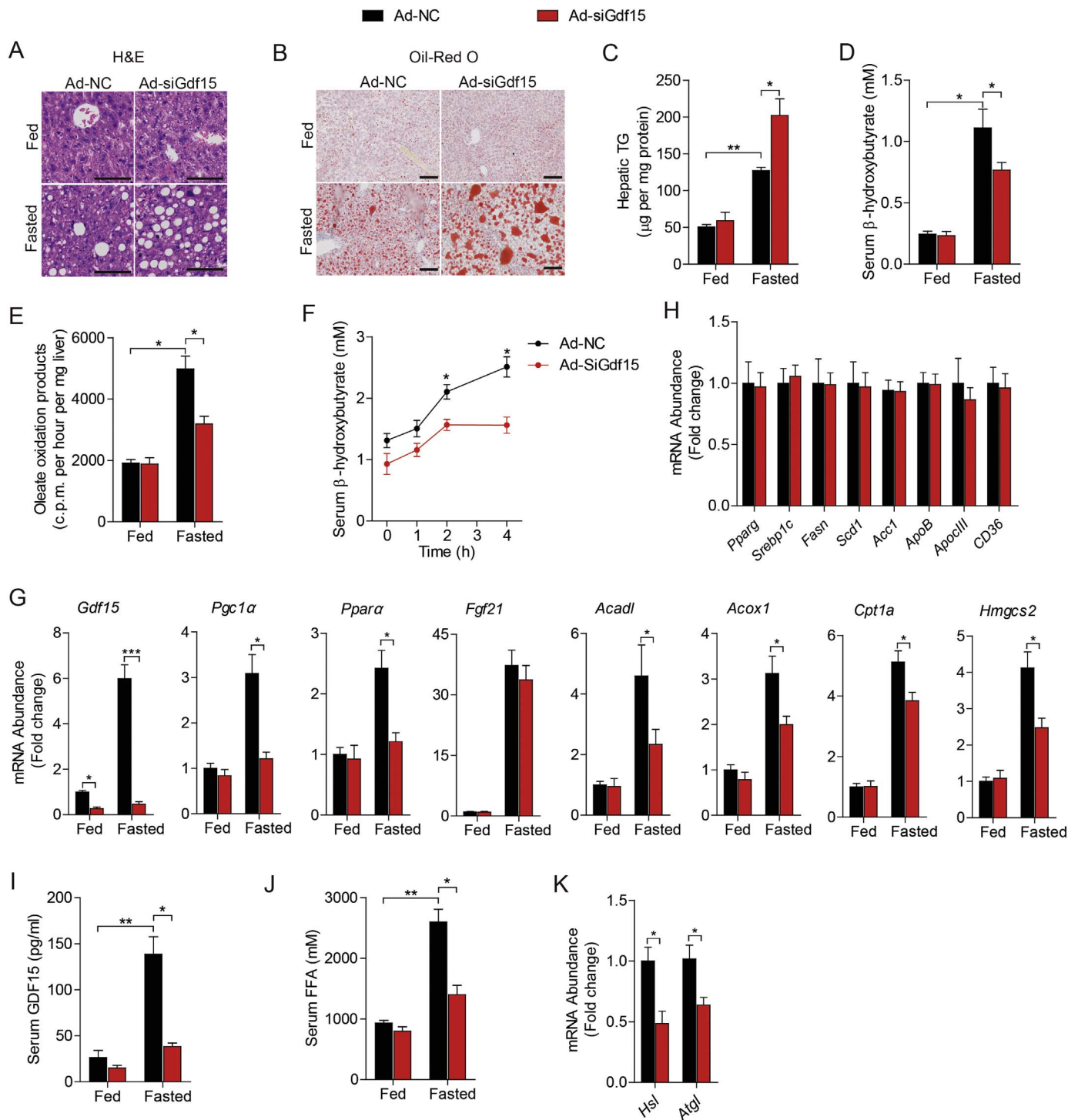
Fig. 3. Abrogation of hepatic GDF15 attenuates fasting-induced fatty acid β-oxidation and ketogenesis. Male C57BL/6 J mice were administered adenovirus expressing negative control siRNA (Ad-NC) or siGdf15 targeted at mouse *Gdf15* mRNA (Ad-siGdf15) at the age of 10 weeks and then subjected for 24-h fasting two weeks later (n = 10 for groups of ad-NC and ad-siGdf15) or fed ad libitum (n = 6 for groups of ad-NC and ad-siGdf15). A-B, Representative images of liver sections stained with H&E (A) and Oil-red O (B). Scale bar is 100 μm. C, Liver contents of triglycerides (TG). D, Serum contents of β-hydroxybutyrate. E, Determination of fatty acid β-oxidation by the using of fresh liver homogenates. F, Serum β-hydroxybutyrate were determined at indicated time points of the fasted mice which were i.p. injected with sodium octanoate. G-H, qRT-PCR analysis of the mRNA abundance of the indicated genes in liver. *Rps18* was used as the internal control. I, ELISA assays determined serum contents of GDF15. J, Serum contents of free fat acids (FFA). K, qRT-PCR analysis of the mRNA abundance of *Hsl* and *Atgl* in gonadal white adipose tissue (gWAT). All data are shown as mean ± s.e.m.. *, $p < .05$; **, $p < .01$ or ***, $p < .001$ by unpaired two-tailed Student's t-test or two-way ANOVA.

(ad-GFP) as control or GDF15 (ad-GDF15) to enforce GDF15 levels in livers (Fig. 6A–B) and circulation (Fig. 6C). In comparison to control mice, with similar body weight and food intake (Fig. S6A–B), ectopic GDF15 resulted in significantly reduced liver weight (Fig. 6D), hepatic contents of TG (Fig. 6E), impaired hepatosteatosis (Fig. 6F-G),

improved NAFLD (Fig. 6H-I) and liver damage (Fig. 6J) in obese mice. Furthermore, GDF15-expressed obese mice exhibited dramatically improved glucose tolerance (Fig. 6K), reduced insulin resistance (Fig. 6L) and hyperinsulinemia (Fig. 6M). As expected, ectopic expression of hepatic GDF15 heightened serum contents of ketones, indicating
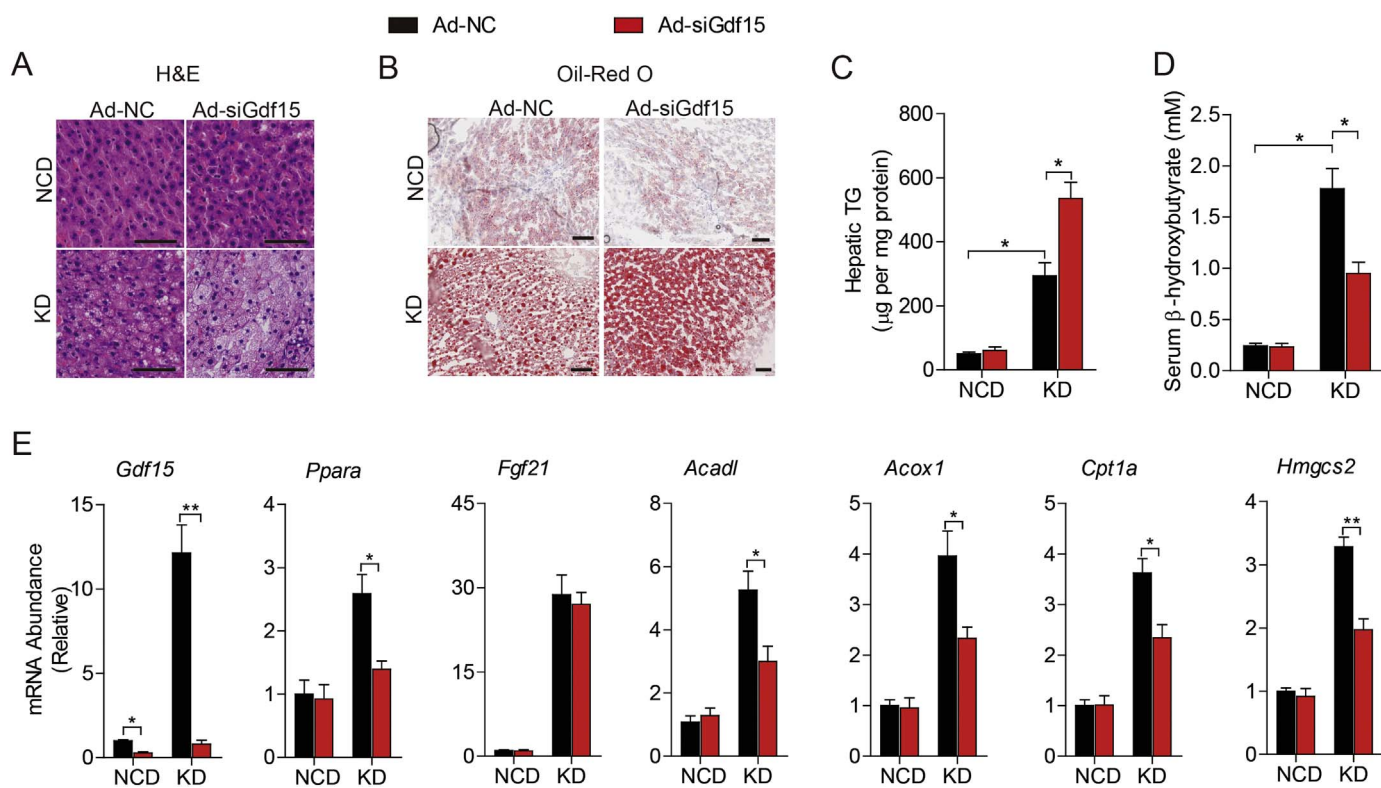
Fig. 4. Ablation of hepatic GDF15 reduces diet-induced ketogenesis. Male C57BL/6 J mice were administered adenovirus expressing negative control siRNA (Ad-NC) or siGdf15 targeted at mouse *Gdf15* mRNA (Ad-siGdf15) at the age of 10 weeks and then fed with ketogenic diet (KD, (n = 8 for groups of ad-NC and ad-siGdf15)) or normal chow diet (NCD) (n = 6 for groups of ad-NC and ad-siGdf15) for 3 days. A-B, Representative images of liver sections stained with H&E (A) and Oil-red O (B). Scale bar is 100 μm. C, Liver contents of TG. D, Serum contents of β-hydroxybutyrate. E, qRT-PCR analysis of the mRNA abundance of the indicated genes in liver. *Rps18* was used as the internal control. All data are shown as mean ± s.e.m.. *, $p < .05$ or **, $p < .01$ by two-way ANOVA.

elevated ketone production of liver (Fig. 6N). Obese mice with higher hepatic GDF15 exhibited dramatic upregulation of genes associated with fatty acids β-oxidation and ketogenesis, including *Ppara, Pgc1a, Cpt1a, Acox* and *Hmgcs2* (Fig. 6O). Additionally, increased hepatic GDF15 didn't alter mRNA levels of genes involved in *de novel* lipogenesis, free fatty acid (FFA) uptake and vLDL secretion in liver (Fig. S6C). Interestingly, although similar serum FFA contents as control (Fig. S6D), micead-GDF15-injected mice had higher mRNA abundances of *Hsl* and *Atgl* in gWAT (Fig. 6P), suggesting that increased circulating GDF15 enhance lipolysis in adipose tissue. These results reveal that increased hepatic GDF15 could alleviate the development of obesity-induced NFALD via promoting hepatic oxidation of lipids.

4. Discussion

Growing studies reveal that elevated GDF15 in blood display a close association with type 2 diabetes, cardiovascular diseases and liver diseases [31–33]. GDF15 is considered as a crucial hormone in regulating lipid and carbohydrate metabolism, and is even to be used as a biomarker for diabetes and cardiovascular diseases [6,14,15]. It still remains elusive the physiological roles of GDF15 in metabolic adaptions and nonalcoholic fatty liver disease (NALFD) development of liver, however. In our present study, *Gdf-15* expression is driven by increased XBP1s and elevated GDF15 enhances hepatic β-oxidation of fatty acids to supply ketones for peripheral tissues and organs upon fasting or ketogenic diet feeding. Abrogation of hepatic GDF15 could impair hepatic fatty acid β-oxidation and ketogenesis in fasted and diabetic mice. Conversely, ectopic expression of hepatic GDF-15 result in reduced hepatic steatosis and improved insulin resistance in obese mice.

GDF15 are implicated in maintaining systemic energy homeostasis. Previous report reveal that human GDF15-transgenic mice could

protect against high fat diet-induced obesity via augmenting thermogenesis, lipolysis and oxidative metabolism in adipose tissue [15]. Furthermore, skeletal muscle-derived GDF15 plays as a myomitokine in governing systemic energy homeostasis [14]. Importantly, GDF15 secreted by hepatocytes acts as an important hepatokine in regulating lipid homeostasis of liver [3,34]. In our study, hepatocyte-expressed GDF15 is indeed needed for activing fatty acid β-oxidation in liver when faced to 24-h fasting (Fig. 3). Notably, deleting carnitine palmitoyltransferase 2 (Cpt2) in liver could lead to enhanced hepatic *Gdf15* expression and serum GDF15 contents, and even higher when the mice were subjected to fasting, suggesting the critical roles of hepatic GDF15 in fatty acid β-oxidation and metabolic adaptions of liver in facing to starvation [3]. Inhibition of GDF15 expression in liver could efficiently reduce the activities of hepatic fatty acid β-oxidation and ketone production via repressing key oxidation-associated genes expression (such as *Ppara, Pgc1a Cpt1a, Acox*1 and *Hmgcs2*) in the livers of fasted mice (Fig. 3), as well as the mice with STZ-induced type 1 diabetes (Fig. 4). As ketoacidosis is one of the most dangerous diabetes complications, inhibition of hepatic GDF15 might be a promising method to control circulating ketone levels in diabetic patients.

In our current study, decreased hepatic GDF15 resulted in reduced oxidative metabolism-associated genes but didn't affect the expression of *Fgf21* in liver. Although PPARα is considered as the main mediator in regulating hepatic *Fgf21* expression, the loss of PPARα didn't cause significant impairment of hepatic *Fgf*21expression in mice subjected to 24-h fast [35], indicating that some other regulators might activate *Fgf21* expression as a compensation of PPARα loss during fasting, i.e. XBP1s [28]. More XBP1s are generated by heightened ER stress in GDF15-deficient liver with higher TG accumulation (data not shown) and subsequently promote *Fgf21* expression, which might diminish the effects of PPARα reduction. Indeed, the underlying molecular metabolism(s) of GDF15 in regulating hepatic fatty acid β-oxidation are
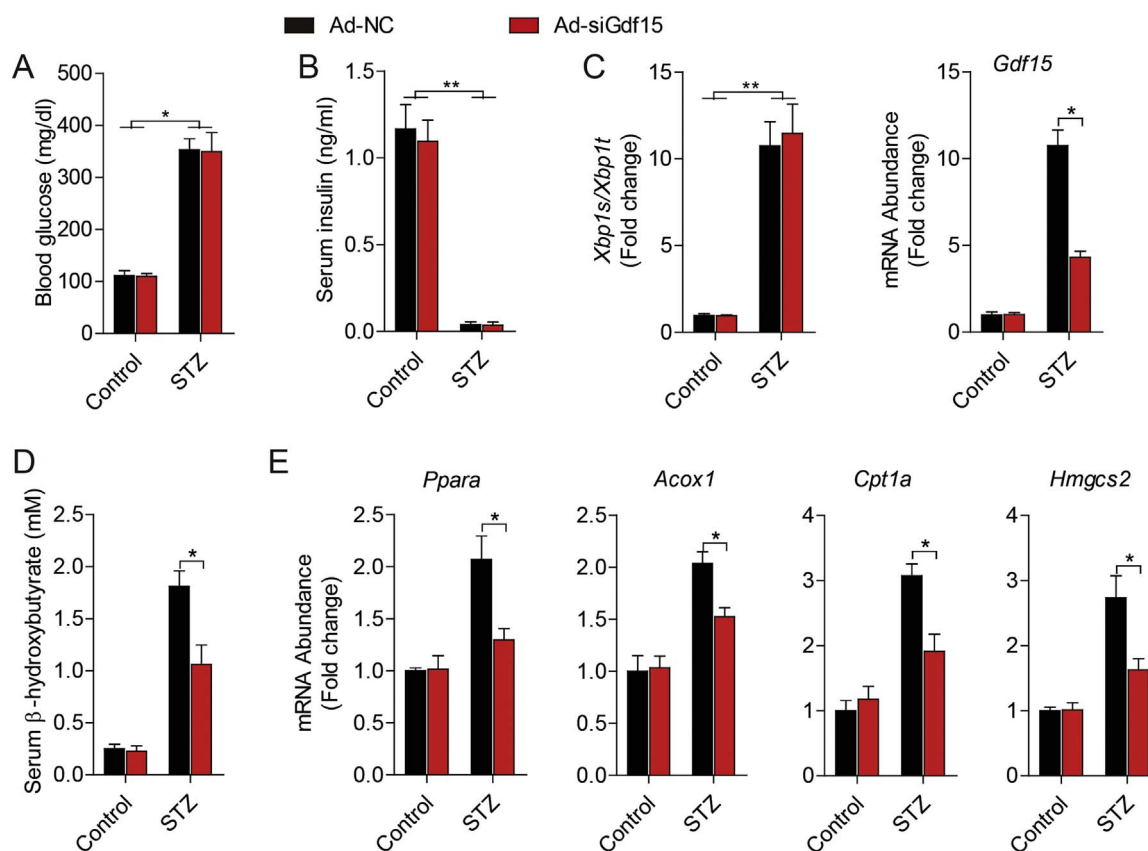
Fig. 5. Loss of hepatic GDF15 impairs the production of ketone in diabetic mice. Male C57BL/6 J mice were administered adenovirus of ad-NC or ad-siGdf15 at the age of 10 weeks and two weeks later, these mice were i.p. injected with saline (Control, n = 6 for groups of ad-NC and ad-siGdf15) or STZ (250 mg per Kg body weight, n = 10 for groups of ad-NC and ad-siGdf15), respectively. A, Blood glucose levels. B, Serum contents of insulin. C, qRT-PCR analysis of Xbp1 splicing and *Gdf15* mRNA abundance in liver. D, Serum contents of β-hydroxybutyrate. E, qRT-PCR analysis of mRNA abundance of indicated genes in liver. *Rps18* was used as the internal control. All data are shown as mean ± s.e.m.. *, $p < .05$ by two-way ANOVA.

needed to be elucidated to help people understand the interrelationships of GDF15 and FGF21 in regulating the complicated processes of liver lipid metabolism.

Circulating GDF15 levels are positively correlated with body weight in human and elevated GDF15 in tissues and blood has been revealed in obese mice [11,14,36,37]. Recently, 3 independent studies demonstrate that GDF15 could bind with high affinity to GDNF family receptor a-like (GFRAL) in neurons to promote weight loss in mice and nonhuman primates, enabling a more comprehensive assessment of GDF15 as a potential pharmacotherapy for the treatment of obesity [38–40]. In our present study, ectopic expression of GDF15 in liver of obese mice could conversely augment lipid catabolism in liver and eventually result in alleviated NAFLD development and improved insulin resistance (Fig. 5), which are in consistent with the metabolic beneficial effects of upregulated GDF15 in Cpt2-deficient mice [34]. Interestingly, we didn't find overexpressed hepatic *Gdf15* affect body weight and calorie uptake of obese mice even circulating GDF15 levels were much higher in ad-GDF15-injected mice (Fig. 6C, Fig. S6A-B). These may be due to the in vivo experiments we did in the *db/db* mice were all completed within 4 weeks after the adenovirus injection.

ER stress is thought to underlie metabolic dysfunctions [41,42], and the UPR pathways are implicated in many metabolic processes [21,26,43]. Previous study has well revealed the crucial role of IRE1α-XBP1s branch of the UPR pathway in orchestrating fatty acid β-oxidation and ketogenesis through activating *Ppara* transcription upon fasting and ketogenic diet feeding [21]. Moreover, accumulative evidences demonstrate that IRE1α-XBP1 pathway controls take part in the regulation of various metabolic processes, such as protein disulphide isomerase (PDI) [44], fatty acid synthase (FAS) or UDP-galactose-4-

epimerase [20], or through non-transcriptional actions such as promoting degradation of the forkhead box O1 transcription factor (FoxO1) [45]. We found that fasting-induced increased activation of IRE1α-XBP1s could drive the transcription of *Gdf15* in liver (Fig. 2). Chung et al. reported that CHOP could activate GDF15 expression in skeletal muscle [14]. As fasting and ketogenic diet show no effects on hepatic *Chop* expression (Fig. S2), we can exclude the possibility of CHOP-regulating *Gdf15* expression in fasted liver, indicating various molecular mechanisms in regulating GDF15 expression in different tissues. Despite of these, increased activation of the UPR pathways in fatty liver also implicates that elevated GDF15 levels of obese mice might be mostly contributed by upregulated XBP1s in liver. To investigate whether classical ER stress could exacerbate *Gdf15* expression in liver, we treat the mice with Tm to induce ER stress in the liver [25]. Interestingly, we found that the Tm treatment could also activate hepatic *Gdf15* expression and serum levels of GDF15, which further indicates the important role of the UPR pathways in Gdf15 expression of liver (Fig. S3). Our results are supported by an independent research work from another lab, which was recently published [46]. Thus, the UPR pathways are critical in controlling hepatic *Gdf15* expression to regulate lipid metabolism of liver. Further studies are needed to elucidate underlying mechanisms of UPR pathways and GDF15 in future.

In summary, our present study reveals a key role of hepatocyate-derived GDF15 in hepatic lipid homeostasis. These findings will be applicable in the clinical treatment and drug discovery for diabetes and NAFLD.
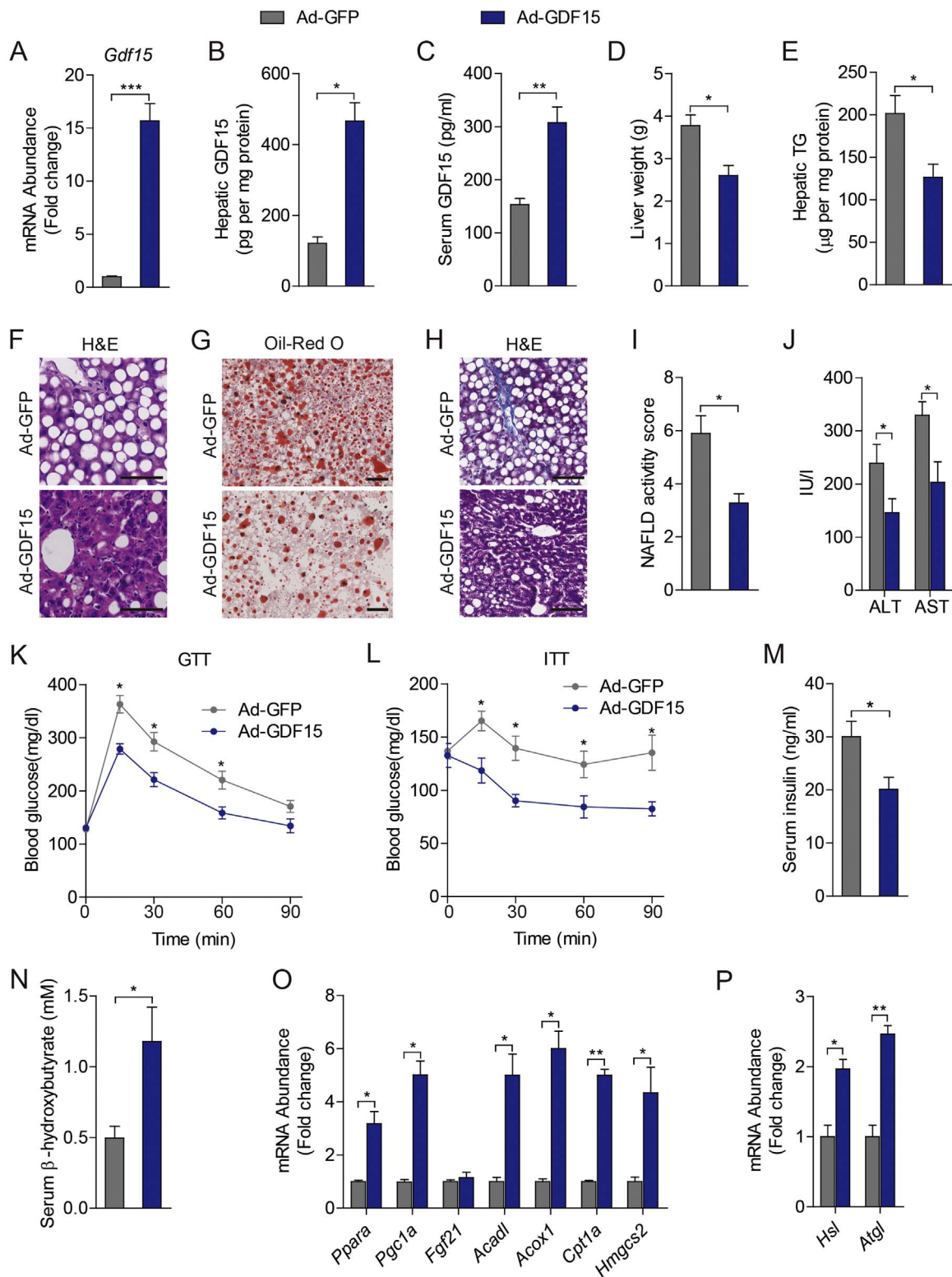
Fig. 6. Elevated hepatic GDF15 reduces obesity-induced hepatosteatosis via enhancing hepatic lipid catabolism. *db/db* mice at 10 weeks of age were administered with adenovirus expressing GFP (Ad) or GDF15 (Ad-GDF15). A, qRT-PCR analysis of mRNA abundance of *Gdf15* in liver. B-C, GDF15 contents in liver (C) and serum (B). D, Liver weight. E, Hepatic TG. F-H, Representative images of liver sections stained with H&E (F), Oil-red O (G) and Masson's trichrome (H). Scale bar is 100 μm. I, NAFLD activity. J, Levels of ALT and AST. K, Glucose tolerance tests (GTT). L, Insulin tolerance tests (ITT). M-N, Serum levels of insulin (M) and β-hydroxybutyrate (N). O-P, qRT-PCR analysis of mRNA abundance of indicated genes in liver (O) and *Hsl* and *Atgl* in gWAT (P). For A, O and P, *Rps18* was used as the internal control. All data are shown as mean ± s.e.m.. *, $p < .05$; **, $p < .01$ or ***, $p < .001$ by unpaired two-tailed Student's *t*-test or two-way ANOVA.

Funding

Data availability statement

The datasets used and/or analyzed during the current study available from the corresponding author on reasonable request.

Authors' contributions

M. Zhang and Y. Tang conceived and designed the studies. M. Zhang, W. Sun and J. Qian conducted most of the experiments and analyzed the data. M. Zhang and Y. Tang wrote the manuscript.

Competing interests

The authors declare no competing financial interests.

Appendix A. Supporting information

Supplementary data associated with this article can be found in the online version at http://dx.doi.org/10.1016/j.redox.2018.01.013.

References

[1] G.F. Cahill Jr., Fuel metabolism in starvation, Annu. Rev. Nutr. 26 (2006) 1–22.

[2] O.E. Owen, A.P. Morgan, H.G. Kemp, J.M. Sullivan, M.G. Herrera, G.F. Cahill Jr., Brain metabolism during fasting, J. Clin. Investig. 46 (10) (1967) 1589–1595.

[3] J. Lee, J. Choi, S. Scafidi, M.J. Wolfgang, Hepatic fatty acid oxidation restrains systemic catabolism during starvation, Cell Rep. 16 (1) (2016) 201–212.

[4] S. Kersten, J. Seydoux, J.M. Peters, F.J. Gonzalez, B. Desvergne, W. Wahli, Peroxisome proliferator-activated receptor alpha mediates the adaptive response to fasting, J. Clin. Investig. 103 (11) (1999) 1489–1498.

[5] M.K. Badman, P. Pissios, A.R. Kennedy, G. Koukos, J.S. Flier, E. Maratos-Flier, Hepatic fibroblast growth factor 21 is regulated by pparalpha and is a key mediator of hepatic lipid metabolism in ketotic states, Cell Metab. 5 (6) (2007) 426–437.

[6] R. Adela, S.K. Banerjee, Gdf-15 as a target and biomarker for diabetes and cardiovascular diseases: a translational prospective, J. Diabetes Res. 2015 (2015) 490842.

[7] H. Johnen, S. Lin, T. Kuffner, D.A. Brown, V.W. Tsai, A.R. Bauskin, et al., Tumor-induced anorexia and weight loss are mediated by the tgf-beta superfamily cytokine mic-1, Nat. Med. 13 (11) (2007) 1333–1340.

[8] M. Yokoyama-Kobayashi, M. Saeki, S. Sekine, S. Kato, Human cdna encoding a novel tgf-beta superfamily protein highly expressed in placenta, J. Biochem. 122 (3) (1997) 622–626.

[9] J. Koopmann, P. Buckhaults, D.A. Brown, M.L. Zahurak, N. Sato, N. Fukushima, et al., Serum macrophage inhibitory cytokine 1 as a marker of pancreatic and other periampullary cancers, Clin. Cancer Res. 10 (7) (2004) 2386–2392.

[10] T. Kempf, R. Horn-Wichmann, G. Brabant, T. Peter, T. Allhoff, G. Klein, et al., Circulating concentrations of growth-differentiation factor 15 in apparently healthy elderly individuals and patients with chronic heart failure as assessed by a new immunoradiometric sandwich assay, Clin. Chem. 53 (2) (2007) 284–291.

[11] Q. Ding, T. Mracek, P. Gonzalez-Muniesa, K. Kos, J. Wilding, P. Trayhurn, et al., Identification of macrophage inhibitory cytokine-1 in adipose tissue and its secretion as an adipokine by human adipocytes, Endocrinology 150 (4) (2009) 1688–1696.

[12] D.A. Brown, S.N. Breit, J. Buring, W.D. Fairlie, A.R. Bauskin, T. Liu, et al., Concentration in plasma of macrophage inhibitory cytokine-1 and risk of cardiovascular events in women: a nested case-control study, Lancet 359 (9324) (2002) 2159–2163.

[13] T. Kempf, E. Bjorklund, S. Olofsson, B. Lindahl, T. Allhoff, T. Peter, et al., Growth-differentiation factor-15 improves risk stratification in st-segment elevation myocardial infarction, Eur. Heart J. 28 (23) (2007) 2858–2865.

[14] H.K. Chung, D. Ryu, K.S. Kim, J.Y. Chang, Y.K. Kim, H.S. Yi, et al., Growth differentiation factor 15 is a myomitokine governing systemic energy homeostasis, J. Cell Biol. 216 (1) (2017) 149–165.

[15] K. Chrysovergis, X. Wang, J. Kosak, S.H. Lee, J.S. Kim, J.F. Foley, et al., Nag-1/gdf-15 prevents obesity by increasing thermogenesis, lipolysis and oxidative metabolism, Int. J. Obes. (Lond.) 38 (12) (2014) 1555–1564.

[16] D. Ron, P. Walter, Signal integration in the endoplasmic reticulum unfolded protein response, Nat. Rev. Mol. Cell Biol. 8 (7) (2007) 519–529.

[17] P. Walter, D. Ron, The unfolded protein response: from stress pathway to homeostatic regulation, Science 334 (6059) (2011) 1081–1086.

[18] M. Schroder, R.J. Kaufman, The mammalian unfolded protein response, Annu. Rev. Biochem. 74 (2005) 739–789.

[19] H. Yoshida, T. Matsui, A. Yamamoto, T. Okada, K. Mori, Xbp1 mrna is induced by atf6 and spliced by ire1 in response to er stress to produce a highly active transcription factor, Cell 107 (7) (2001) 881–891.

[20] Y. Deng, Z.V. Wang, C. Tao, N. Gao, W.L. Holland, A. Ferdous, et al., The xbp1s/gale axis links er stress to postprandial hepatic metabolism, J. Clin. Investig. 123 (1) (2013) 455–468.

[21] M. Shao, B. Shan, Y. Liu, Y. Deng, C. Yan, Y. Wu, et al., Hepatic ire1alpha regulates fasting-induced metabolic adaptive programs through the xbp1s-pparalpha axis signalling, Nat. Commun. 5 (2014) 3528.

[22] T. Mao, M. Shao, Y. Qiu, J. Huang, Y. Zhang, B. Song, et al., Pka phosphorylation couples hepatic inositol-requiring enzyme 1alpha to glucagon signaling in glucose metabolism, Proc. Natl. Acad. Sci. USA 108 (38) (2011) 15852–15857.

[23] A.H. Lee, E.F. Scapa, D.E. Cohen, L.H. Glimcher, Regulation of hepatic lipogenesis by the transcription factor xbp1, Science 320 (5882) (2008) 1492–1496.

[24] D.T. Rutkowski, J. Wu, S.H. Back, M.U. Callaghan, S.P. Ferris, J. Iqbal, et al., Upr pathways combine to prevent hepatic steatosis caused by er stress-mediated suppression of transcriptional master regulators, Dev. Cell 15 (6) (2008) 829–840.

[25] K. Zhang, S. Wang, J. Malhotra, J.R. Hassler, S.H. Back, G. Wang, et al., The unfolded protein response transducer ire1alpha prevents er stress-induced hepatic steatosis, EMBO J. 30 (7) (2011) 1357–1375.

[26] B. Shan, X. Wang, Y. Wu, C. Xu, Z. Xia, J. Dai, et al., The metabolic er stress sensor ire1alpha suppresses alternative activation of macrophages and impairs energy expenditure in obesity, Nat. Immunol. 18 (5) (2017) 519–529.

[27] K. Yamamoto, H. Yoshida, K. Kokame, R.J. Kaufman, K. Mori, Differential contributions of atf6 and xbp1 to the activation of endoplasmic reticulum stress-responsive cis-acting elements erse, upre and erse-ii, J. Biochem. 136 (3) (2004) 343–350.

[28] S. Jiang, C. Yan, Q.C. Fang, M.L. Shao, Y.L. Zhang, Y. Liu, et al., Fibroblast growth factor 21 is regulated by the ire1alpha-xbp1 branch of the unfolded protein response and counteracts endoplasmic reticulum stress-induced hepatic steatosis, J. Biol. Chem. 289 (43) (2014) 29751–29765.

[29] S. Sengupta, T.R. Peterson, M. Laplante, S. Oh, D.M. Sabatini, Mtorc1 controls fasting-induced ketogenesis and its modulation by ageing, Nature 468 (7327) (2010) 1100–1104.

[30] P.J. Blackshear, K.G. Alberti, Experimental diabetic ketoacidosis. Sequential changes of metabolic intermediates in blood, liver, cerebrospinal fluid and brain after acute insulin deprivation in the streptozotocin-diabetic rat, Biochem. J. 138 (1) (1974) 107–117.

[31] H. Zhang, W. Zhang, X. Tu, Y. Niu, X. Li, L. Qin, et al., Elevated serum growth differentiation factor 15 levels are associated with thyroid nodules in type 2 diabetes aged over 60 years, Oncotarget 8 (25) (2017) 41379–41386.

[32] M.Y. Shin, J.M. Kim, Y.E. Kang, M.K. Kim, K.H. Joung, J.H. Lee, et al., Association between growth differentiation factor 15 (gdf15) and cardiovascular risk in patients with newly diagnosed type 2 diabetes mellitus, J. Korean Med. Sci. 31 (9) (2016) 1413–gdf1418.

[33] E.S. Lee, S.H. Kim, H.J. Kim, K.H. Kim, B.S. Lee, B.J. Ku, Growth differentiation factor 15 predicts chronic liver disease severity, Gut Liver 11 (2) (2017) 276.

[34] J. Lee, J. Choi, E.S. Selen Alpergin, L. Zhao, T. Hartung, S. Scafidi, et al., Loss of hepatic mitochondrial long-chain fatty acid oxidation confers resistance to diet-induced obesity and glucose intolerance, Cell Rep. 20 (3) (2017) 655–667.

[35] Q. Gao, Y. Jia, G. Yang, X. Zhang, P.C. Boddu, B. Petersen, et al., Pparalpha-deficient ob/ob obese mice become more obese and manifest severe hepatic steatosis due to decreased fatty acid oxidation, Am. J. Pathol. 185 (5) (2015) 1396–1408.

[36] V.W. Tsai, L. Macia, C. Feinle-Bisset, R. Manandhar, A. Astrup, A. Raben, et al., Serum levels of human mic-1/gdf15 vary in a diurnal pattern, do not display a profile suggestive of a satiety factor and are related to bmi, PLoS One 10 (7) (2015) e0133362.

[37] F. Verdeguer, M.S. Soustek, M. Hatting, S.M. Blattler, D. McDonald, J.J. Barrow, et al., Brown adipose yy1 deficiency activates expression of secreted proteins linked to energy expenditure and prevents diet-induced obesity, Mol. Cell. Biol. 36 (1) (2015) 184–196.

[38] S.E. Mullican, X. Lin-Schmidt, C.N. Chin, J.A. Chavez, J.L. Furman, A.A. Armstrong, et al., Gfral is the receptor for gdf15 and the ligand promotes weight loss in mice and nonhuman primates, Nat. Med. (2017).

[39] L. Yang, C.C. Chang, Z. Sun, D. Madsen, H. Zhu, S.B. Padkjaer, et al., Gfral is the receptor for gdf15 and is required for the anti-obesity effects of the ligand, Nat. Med. (2017).

[40] P.J. Emmerson, F. Wang, Y. Du, Q. Liu, R.T. Pickard, M.D. Gonciarz, et al., The metabolic effects of gdf15 are mediated by the orphan receptor gfral, Nat. Med. (2017).

[41] G.S. Hotamisligil, Endoplasmic reticulum stress and the inflammatory basis of metabolic disease, Cell 140 (6) (2010) 900–917.

[42] H. Malhi, R.J. Kaufman, Endoplasmic reticulum stress in liver disease, J. Hepatol. 54 (4) (2011) 795–809.

[43] S. Fu, S.M. Watkins, G.S. Hotamisligil, The role of endoplasmic reticulum in hepatic lipid homeostasis and stress signaling, Cell Metab. 15 (5) (2012) 623–634.

[44] S. Wang, Z. Chen, V. Lam, J. Han, J. Hassler, B.N. Finck, et al., Ire1alpha-xbp1s induces pdi expression to increase mtp activity for hepatic vldl assembly and lipid homeostasis, Cell Metab. 16 (4) (2012) 473–486.

[45] Y. Zhou, J. Lee, C.M. Reno, C. Sun, S.W. Park, J. Chung, et al., Regulation of glucose homeostasis through a xbp-1-foxo1 interaction, Nat. Med. 17 (3) (2011) 356–365.

[46] D. Li, H. Zhang, Y. Zhong, Hepatic gdf15 is regulated by chop of the unfolded protein response and alleviates nafld progression in obese mice, Biochem. Biophys. Res. Commun. (2017).